論文の内容の要旨

論文題目：Atomic and Molecular Dipolar Fermi Gas
and Nuclear Meson Condensations

(原子・分子双極子フェルミ気体と中間子凝縮)

氏　名　　前田　賢志

In this thesis, we study, as an analog of meson condensation in neutron matter, an inhomogeneous ground state in a many-body system of two-component Fermi gas with a dipole-dipole interaction and a contact interaction. We investigate the phase diagram of the dipolar Fermi gas as functions of dimensionless parameters related to the dipole-dipole and contact interactions. Novel quantum phases which may appear in this system are of current interest, because experiments are beginning to explore the physics of fermionic gases with strong dipole-dipole interactions.

The most advantageous structure of the dipolar Fermi system is determined by a competition among the dipolar interaction which favors magnetization (spin polarization) varying in direction in space, the short-range repulsions which favor aligned spins, and the particle kinetic energies which favor spatially uniform structures. Inspired by the extended alternating layer spin (EALS) state in the study of ρ^0 meson condensation, we first introduce an antiferrrosmectic-C (AFSC) state as a variational ground state of the dipolar Fermi system. The AFSC state has a one-dimensional periodic structure in which the fermions localize in layers with their pseudospin direction aligned parallel to the layers, and staggered layer by layer. Figure 1 shows the structure of the AFSC state. The expectation values of the number density and local magnetization in the AFSC state are given by

$$\begin{aligned} \langle n(\vec{r})\rangle &= \frac{nd}{b\sqrt{\pi}} \sum_{\ell=-\infty}^{\infty} e^{-(z-d\ell)^2/b^2}, \\ \langle M_x(\vec{r})\rangle &= -\frac{\mu n d}{b\sqrt{\pi}} \sum_{\ell=-\infty}^{\infty} (-1)^{\ell} e^{-(z-d\ell)^2/b^2}, \end{aligned}$$

and $\langle M_y(\vec{r})\rangle = \langle M_z(\vec{r})\rangle = 0$, where d is the distance between neighboring layers and b is the width of the layer determined so as to minimize the total energy density. We explicitly derive the energy

density of the AFSC phase in units of the energy density of the free Fermi gas

$$\begin{aligned}\frac{\mathcal{E}(\Gamma,\alpha)}{\frac{3}{5}n\epsilon_F} &= \frac{10}{3(3\pi)^{2/3}}\Gamma^{1/3}\alpha^{2/3}+\frac{5}{3(3\pi)^{2/3}}\Gamma^{1/3}\alpha^{-1/3} \\ &\quad -\frac{20\pi}{3}\lambda_d\sum_{j=1}^{\infty}e^{-(2j-1)^2\pi^2/2\Gamma}\left\{\frac{1}{3}-F(\alpha)\right\} \\ &\quad +\frac{5}{6}\lambda_s\left\{\frac{1}{2}-\sum_{j=1}^{\infty}\left[e^{-(2j-1)^2\pi^2/2\Gamma}-e^{-2j^2\pi^2/\Gamma}\right]\right\}.\end{aligned}$$

The first term on the right is the one-dimensional zero-point energy in the z-direction, and the second term is the two-dimensional kinetic, or Fermi energy within a layer. The third term arises from the dipole-dipole interaction, with $1/3$ and $-F(\alpha)$ the direct and exchange contributions, respectively, where

$$F(\alpha) = \alpha\int_0^{\infty}\mathrm{d}s J_1^2\left(\sqrt{2s/\alpha}\right)e^s\left\{\frac{2s+1}{s}K_0(s)-2K_1(s)\right\},$$

and J_i and K_i are the Bessel functions of the first kind and second kind, respectively. The dimensionless constants are $\lambda_d = n\mu^2/\epsilon_{_F}, \lambda_s = ng/\epsilon_{_F}$ with the dipolar coupling constant μ and the short-range coupling constant g. The final term is the effect of the contact interaction.

In constructing the phase diagram as functions of the short range interaction, measured by λ_s, and the dipole-dipole interaction, measured by λ_d, as shown in Fig. 2, we compare the minimum of $\mathcal{E}(\Gamma,\alpha)$ with the energy of the interacting Fermi gas phase and with that of the fully polarized ferronematic state. The phase diagram is composed of five distinct regions; (a) the Fermi gas phase, which has a spherical Fermi surface with equal population of both species, (b) the phase with weak spatially varying magnetization, (c) the AFSC phase which has a cylindrical Fermi surface with equal average population, (d) the ferronematic phase which has only a single species, with a spheroidal Fermi surface, and (e) an unstable region. We find that the AFSC phase dominates a wide region of the phase diagram, and that the AFSC phase may be observed in experiments of ultracold fermionic gases with strong dipole-dipole interactions.

We also discuss the generalization of our model with the use of the diagonal and off-diagonal dipole transition moments, so that it becomes suitable for the ultracold atomic/molecular experiments.

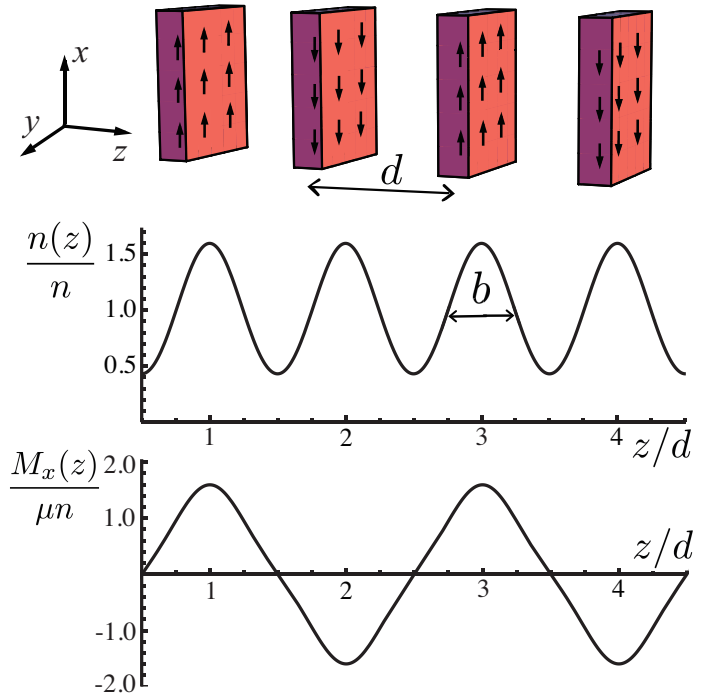

Figure 1: The uppermost panel illustrates the magnetization profile, and the lower two panels the spatial distribution along z-direction of the normalized number density and magnetization in the AFSC state. This is Fig. 3.1 in the thesis.

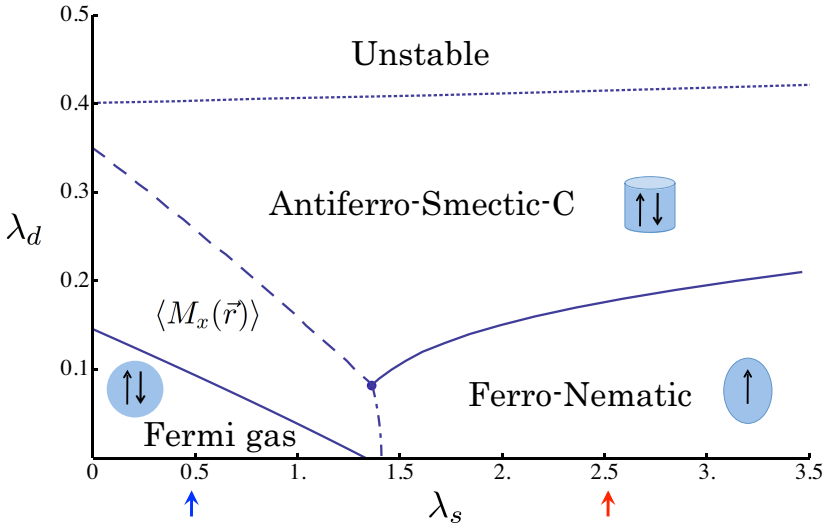

Figure 2: Schematic phase diagram of dipolar fermions as a function of λ_s and λ_d, showing the Fermi gas phase, the ferronematic phase, the onset of spatially varying magnetization and antiferrosmectic-C phase. The dashed line shows where the AFSC phase becomes favorable compared with the uniform unmagnetized interacting Fermi gas, and the dash-dot line the transition between the uniform Fermi gas and the ferronematic phase. Beyond the upper dotted line the system becomes unstable against collapse. This is Fig. 3.10 in the thesis.